A Sea-Surface Radiation Data Set for Climate Applications in the Tropical Western Pacific and South China Sea

Ming-Dah Chou, Pui-King Chan[1], and Michael M.-H. Yan[2]
Laboratory for Atmospheres
NASA Goddard Space Flight Center
Greenbelt, Maryland
USA

1. Introduction

Over tropical oceans, approximately 20% of the incoming solar radiation at the top of the atmosphere is reflected by the ocean-atmosphere system, 25% is absorbed in the atmosphere, and 55% is absorbed by the ocean. Surface radiation over the ocean is an essential component of the Earth's radiation budgets in atmospheric and oceanic studies. The information on surface radiation is important for understanding the processes that affect the sea surface temperature (e.g. *Chou et al.*, 2000). It can also serve as a boundary condition for model simulations of oceanic general circulation.

Starting from January 1998, we have been receiving Japan's Geostationary Meteorological Satellite 5 (GMS-5) radiances at NASA Goddard Space Flight Center on daily basis. The surface solar and thermal infrared radiation are retrieved from the GMS-measured albedo in the visible spectral channel and the brightness temperature in the infrared window. This surface radiation data set covers the region 40°S-40°N, 90°E-170°W. It has a temporal resolution of 1 day and a spatial resolution of 0.5°x0.5° latitude-longitude. We use this surface radiation data set to investigate the effect of El Nino on the surface radiation budget in the tropical western Pacific (TWP) and the South China Sea (SCS). Combined with the solar radiative flux at the top of the atmosphere derived from the Earth's Radiant Energy System (CERES) measurements (Wielicki, et al., 1996), this data set is also used to investigate the effect of clouds on the solar heating of the atmosphere.

2. Derivation and Validation of Surface Radiation

The GMS-5 satellite is positioned above the Equator and 140°E longitude. It measures the Earth's emitted and reflected radiances at 4 narrow spectral channels. The temporal resolution is 1 hr and the spatial resolution is 5 km at the sub-satellite point.

Following Chou et al. (1998), the surface downward solar flux, $S_s^{\downarrow}$, is related to the GMS-measured albedo, α_v, in the visible spectral region centered at 0.7 μm,

$$S_s^{\downarrow} = Q_o \mu_o \tau(\alpha_v, \mu_o) \qquad (1)$$

where μ_o is the cosine of the solar zenith angle, $Q_o\mu_o$ is the incoming solar radiation at the the top of the atmosphere (TOA), τ is the mean atmospheric transmittance of the entire solar spectrum. The surface downward infrared flux is computed from the following empirical relationship,

$$F_s^{\downarrow}=(502-0.464\,T_b-6.75w+0.0565wT_b)\,(T_s/T_o)^4 \qquad (2)$$

where w is the column water vapor amount, T_b is the GMS-measured brightness temperature in the 11-μm window channel, T_s is the sea surface temperature, and T_o=302.1K. Units are g cm^{-2} for w and K for T_b and T_s. The transmission table in Equation (1) and the regression coefficients in Equation (2) were derived based on the surface solar and infrared fluxes measured at 6 sites on islands, research ships, and a buoy during the TOGA COARE Intensive Observing Period.

---

[1] Universities Space Research Association, Seabrook, MD 20706.

[2] Science Systems and Applications, Inc., Lanham, MD 20706.

The Atmospheric Radiation Measurement (ARM) program of the US Department of Energy established an Atmospheric Radiation and Cloud Station (ARCS) in the TWP to measure and study clouds, radiation, and atmospheric properties [*Mather et al.*, 1998]. The GMS-retrieved fluxes are validated against the radiative fluxes measured at this site. Figure 1 shows daily variations of the downward solar fluxes, $S_s^{\downarrow}$, measured at the Manus site (solid curve) and retrieved from GMS albedo measurements (dashed curve). The time series covers a total of 15 months from January 1998 to March 1999. Generally, the two curves follow each other very well. Averaged over the entire 15-month period, $S_s^{\downarrow}$ is 224 W m^{-2} from surface measurements and 231 W m^{-2} from satellite retrievals. The bias is 7 W m^{-2}. The rms difference of the daily $S_s^{\downarrow}$ is 30.3 W m^{-2}. This agreement is very good in view of the spatial inconsistency between satellite and surface measurements, as well as the potential error in surface radiometric measurements.

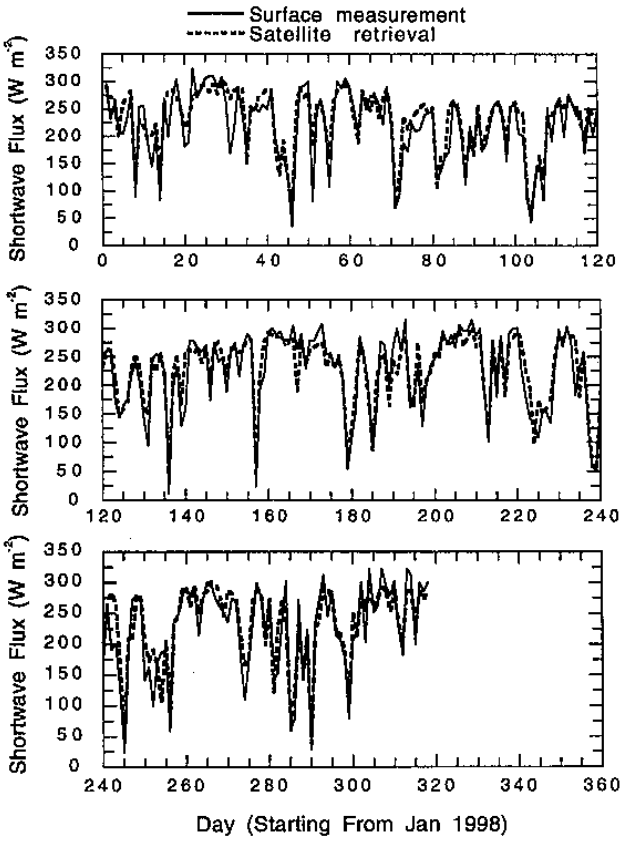

Figure 1. Daily variations of the surface downward SW flux, $S_s^{\downarrow}$, measured at the Manus island and retrieved from GMS-5 albedo measurements during January 1998-March 1999.

Figure 2 shows daily variations of the downward infrared fluxes, $F_s^{\downarrow}$, measured at the Manus ARCS site (solid curve) and retrieved from GMS brightness-temperature measurements (dashed curve). The agreement between the measured and the retrieved $F_s^{\downarrow}$ is very good. Averaged over the 15 months, $F_s^{\downarrow}$ is 423 W m^{-2} from surface measurements and 425 W m^{-2} from satellite retrievals. The rms difference of the daily $F_s^{\downarrow}$ is only 6.6 W m^{-2}.

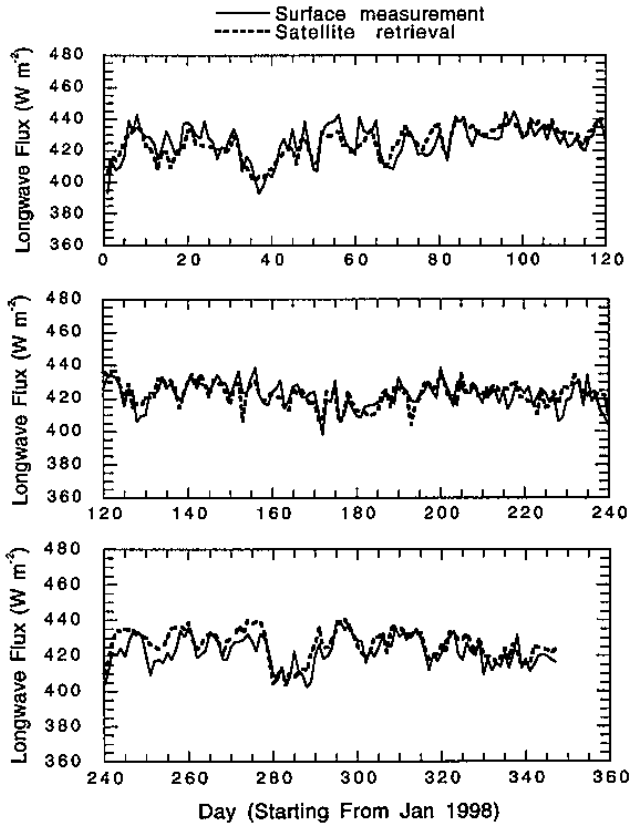

Figure 2. Daily variations of the surface downward LW flux, $F_s^{\downarrow}$, measured at Manus island and retrieved from GMS-5 brightness-temperature measurements.

We have also compared the surface solar radiation retrieved from GMS-5 radiance measurements with the radiometric measurements of fluxes at Dungsha during the South China Sea Monsoon Experiment (SCSMEX). Figure 3 shows daily variations of $S_s^{\downarrow}$ measured at Dungsha (solid curve) and retrieved from GMS-measured albedo (dashed). The two sets of data follow each other very well. Averaged over the 35 days, $S_s^{\downarrow}$ is 211 W m^{-2} from surface measurements and 214 W m^{-2} from

satellite retrievals. The rms difference of the daily SW fluxes is only 17 W m^{-2}.

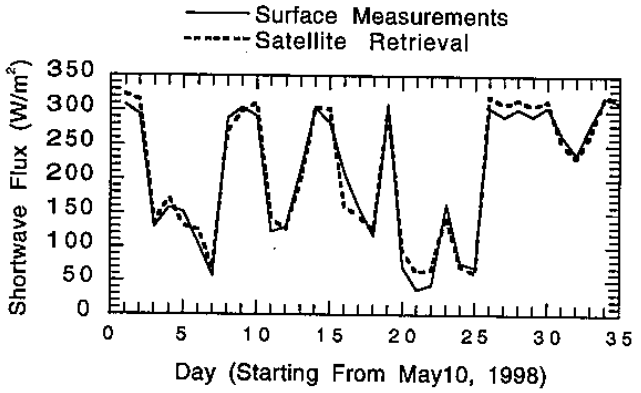

Figure 3. Daily variations of the surface downward SW flux, $S_s^{\downarrow}$, measured at Dungsha island and retrieved from GMS-5 albedo measurements during the SCSMEX IOP (May-June 1998).

3. Spatial and Interannual Variation

The sea surface solar and infrared fluxes have been derived for a period of 20 months from January 1998 to August 1999. The first few months of the year 1998 are in the later phase of the 1997-1998 El Nino. Clouds in the strong convective maritime continents are much reduced compared to the first few months of the year 1999, whereas clouds in the equatorial region east of the dateline increases significantly. Figure 4 shows that corresponding to changes in clouds, the surface net downward radiation increases significantly during the El Nino (February 1998) in the neighborhood of maritime continents and south of the Equator, where the intertropical convergence zone (ITCZ) is located during the Southern Hemispheric summer. Regions of enhanced heating with a magnitude >30 W m^{-2} is wide spread. The net surface heating in the equatorial region east of the dateline decreases by > 60 W m^{-2}, in accordance with the eastward shift of the convection center. These changes are expected to have a large impact on the distribution of sea surface temperature and the oceanic and atmospheric circulations.

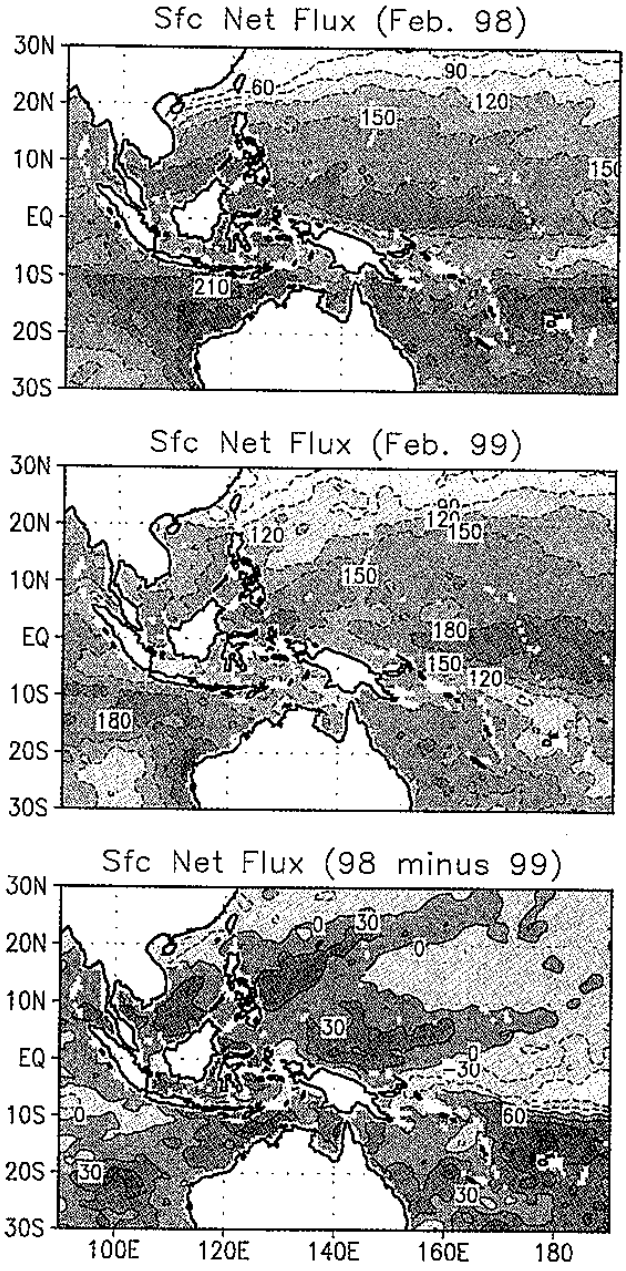

Figure 4. Spatial distribution of the surface net downward radiative (solar+infrared) flux in February 1998 (upper panel), February 1999 (middle panel), and the difference between the two months (lower panel). Units are W m^{-2}.

The South China Sea summer monsoon system is an important component of the East and Southeast Asian climate. Improving the understanding of physical processes and evolution of the monsoon system are among the objectives of the SCSMEX conducted in May and June of 1998 (Lau et al., 2000). The cloud systems associated with the onset, transition, and break stages of the monsoon directly

affect the surface radiative heating, which in turn feedback to affect the dynamics of the monsoon. Figures 5 shows that the surface radiative heating of the South China Sea in May 1998 is smaller by 60 W m^{-2} than May 1999. The onset of the East Asian summer monsoon normally occurs in the month of May. The large change in the radiative heating as shown in the figure is expected to have a significant impact on the onset and evolution of the East Asian summer monsoon.

4. Atmospheric Solar Heating

Clouds cool the Earth by reflecting solar radiation back to space but heat the atmosphere by absorbing solar radiation. It has long been an issue concerning whether the net effect of clouds is to cool or to heat the atmosphere. Radiative transfer calculations show that clouds nearly have no effect on the atmospheric heating, but observation indicates heating of the atmosphere. This issue raises a very important question on the reliability of radiative transfer calculations, which is bound to have a critical impact on remote sensing and climate studies.

The effect of clouds on the solar heating of the atmosphere, Q, is computed using the surface fluxes retrieved from GMS albedo measurements and the fluxes at the top of the atmosphere taken from the CERES ES-4 data archive. The atmospheric solar heating in the tropical western Pacific and the South China Sea are given in Table 1. The magnitudes of Q vary only slightly between the two regions. It is ~100 W m^{-2} for the all-sky solar heating and ~ 80 W m^{-2} for the clear-sky solar heating. Thus, clouds enhance the atmospheric solar heating, or cloud radiative forcing (CRF), by ~ 20 W m^{-2}.

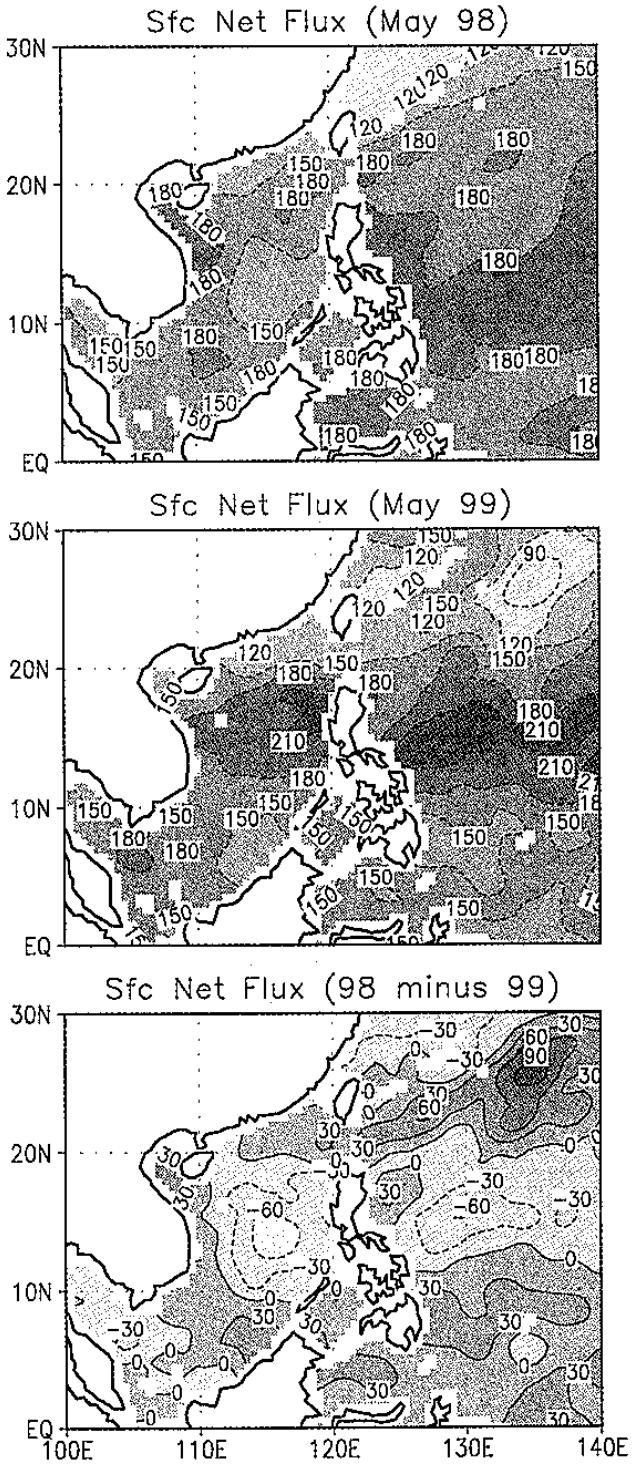

Figure 5. Same as Figure 4, except for May 1998 and May 1999.

Table 1. The all- and clear-sky atmospheric solar heating, and the cloud radiative forcing in the tropical western Pacific (TWP) and the South China Sea (SCS). Units are W m^{-2}.

	TWP	SCS
All-Sky	100.2	106.7
Clear-Sky	77.5	82.5
CRF	22.7	24.2

5. Summary

The sea surface solar and infrared radiative fluxes have been retrieved from the radiances measured by GMS-5 and validated with the radiometric measurements at Manus island in the Pacific warm pool and Dungsha island in the South China Sea. The data set is used to study the effect of El Nino and East Asian Summer monsoon on the heating of the ocean. Interannual variations of clouds associated with El Nino and the East Asian Summer monsoon have a large impact on the radiative heating of the ocean, which exceeds 40 W m^{-2} over large areas. This surface radiation data set is also used to study the impact of clouds on the solar heating of the atmosphere. Clouds have an effect of enhancing the atmospheric solar heating by ~20 W m^{-2} in the tropical western Pacific and the South China Sea. This result is important for resolving the current issue on the accuracy of solar radiation calculations in both clear and cloudy atmospheres.

REFERENCES

Chou, M.-D., W. Zhao and S.-H. Chou, 1998: Radiation budgets and cloud radiative forcing in the Pacific warm pool during TOGA COARE. *J. Geophys. Res., 103*, 16967-16977.

Chou, S.-H., W. Zhao, and M.-D. Chou, 2000: Surface heat budgets and sea surface temperature in the Pacific warm pool during TOGA COARE. *J. Climate, 13*, 634-649.

Lau, K. M., Y. Ding, J. T. Wang, R. Johnson, T. Keenan, R. Cifelli, J. Gerlach, O. Thiele, T. Rickenbach, S. C. Tsay, and P. H. Lin, 2000: A report of the field operations and early results of the South China Sea Monsoon Experiment (SCSMEX). *Bull. Amer. Meteor. Soc.*

Mather, J. H., T. P. Ackerman, W. E. Clements, F. J. Barnes, M. D. Ivey, L. D. Hatfield, and R. M. Reynolds, 1998: An atmospheric radiation and cloud station in the tropical western Pacific. *Bull. Amer. Met. Soc., 79*, 627-642.

Wielicki, B. A., B. R. Barkstrom, E. F. Harrison, R. B. Lee III, G. L. Smith, and J. E. Cooper, 1996: Clouds and the Earth's Radiant Energy System (CERES): An earth observing system experiment. *Bull. Amer. Meteor. Soc., 77*, 853-868.